Journal of Crystal Growth 378 (2013) 222–225

Contents lists available at SciVerse ScienceDirect

Journal of Crystal Growth

journal homepage: www.elsevier.com/locate/jcrysgro

# Growth evolution and magneto-optical characteristics of self-assembled ZnTe/ZnMnSe quantum dots

Ling Lee [a,*], Wen-Chung Fan [b], Kun-Feng Chien [b], An-Jye Tzou [b], Wu-Ching Chou [b,*]

[a] Center of Nanoscience and Technology, Tunghai University, Taichung, Taiwan, Republic of China
[b] Department of Electrophysics, National Chiao Tung University, Hsinchu, Taiwan, Republic of China

ARTICLE INFO

Available online 10 November 2012

*Keywords:*
A1. Nanostructures
A3. Molecular beam epitaxy
B1. Zinc compounds
B2. Magneto-optic materials

ABSTRACT

The growth evolution and the magneto-optical characteristics of the self-assembled single-layer ZnTe/ZnMnSe quantum dots grown by molecular beam epitaxy were investigated. As the ZnTe coverage is above 2.0 monolayers, a Stranski–Krastanov growth process is observed with a significantly increased dot density on top of two-dimensional plateaus. As the coverage exceeds 2.7 monolayers, ripened dots dominate instead. Furthermore, a saturated degree of circular polarization of 76% at applied magnetic field of 4 T and the formation of magnetic polarons with a formation time of 7.4 ns were demonstrated.


## 1. Introduction

Recently dilute magnetic semiconductors (DMS) continue to receive attentions for spintronics [1–3]. In particular, magnetic quantum dots (QD) are of great interest because the control and manipulation of spin are superior to those of bulk and epilayer [4]. For example, we have reported a strong spin polarization at 10 K in the type-II ZnMnTe/ZnSe stacked QD [5,6]. The spatially separated electrons and holes in the type-II band structure provide an advantage of the long spin dephasing time [7]. On the other hand, non-magnetic QD embedded in a magnetic matrix also play as an important candidate for the development of spintronic devices. However, although a stronger polarization of the type-I aligned QD has been demonstrated [8], research on the type-II system is still rare. In this article, self-assembled single-layer ZnTe QD on magnetic ZnMnSe buffer layer were successfully achieved by molecular beam epitaxy (MBE). In addition to the studies on growth evolution, magneto-optical measurements were carried out to investigate the spin polarization and the formation of magnetic polarons (MP).

## 2. Experimental methods

The single-layer ZnTe/ZnMnSe QD were grown on GaAs(100) substrate by a Vecco Applied EPI 620 MBE system at 300 °C. The effusion cell temperatures of Zn, Mn, Se, and Te were fixed at 294, 695, 178, and 310 °C, respectively. Prior to growth, the substrate was etched in a $H_2O_2$:$NH_4OH$:$H_2O$ (1:5:50) solution, rinsed in flowing de-ionized water, dried with purified $N_2$ gas, and desorbed in the MBE chamber in sequence. The growth started from a ZnSe buffer layer and was followed by a 50-nm-thick ZnMnSe barrier layer. The Mn content in the barrier layer was extrapolated from its band gap energy. According to the dependence of band gap energy on Mn incorporation [9], the energy value of 2.790 eV indicates a Mn composition of about 5%. Immediately after the barrier layer, an alternating supply method was performed to deposit ZnTe with a growth rate of 0.03 nm/s. By a careful control of growth duration, ZnTe with coverage of 2.0, 2.2, 2.4, 2.7 and 3.0 monolayers (ML) were fabricated. The morphological properties were measured by tapping-mode atomic force microscopy (AFM).

For the magneto-optical investigations, capped specimens were fabricated with identical growth condition and followed by a 50-nm-thick ZnMnSe capping layer on top. The photoluminescence (PL) measurement was operated at 10 K, in which signals were excited by a Helium–Cadmium laser at 325 nm, analyzed by a Horiba Jobin-Yvon iHR550 0.5-m monochromator and detected by an $LN_2$-cooled charge-coupled device with an energy resolution of 0.3 meV. The magneto-PL spectra were taken in the Faraday geometry in an optical magnet cryostat, in which the polarized signals were extracted by using a combination of a quarter wave plate and a linear polarizer in front of the monochromator. For the time-resolved PL, the signals were excited by a GaN pulsed laser diode at 405 nm, and detected by using a fast photomultiplier tube and a time-correlated single photon counting technique with an overall time resolution of ~0.2 ns.

## 3. Results and discussion

Fig. 1(a) to (e) shows the AFM images of uncapped specimens with ZnTe coverage ranged between 2.0 and 3.0 ML. At both ends

* Corresponding authors.
*E-mail addresses:* leeling@thu.edu.tw (L. Lee), wuchingchou@mail.nctu.edu.tw (W.-C. Chou).

0022-0248/$ - see front matter © 2012 Elsevier B.V. All rights reserved.
http://dx.doi.org/10.1016/j.jcrysgro.2012.11.009

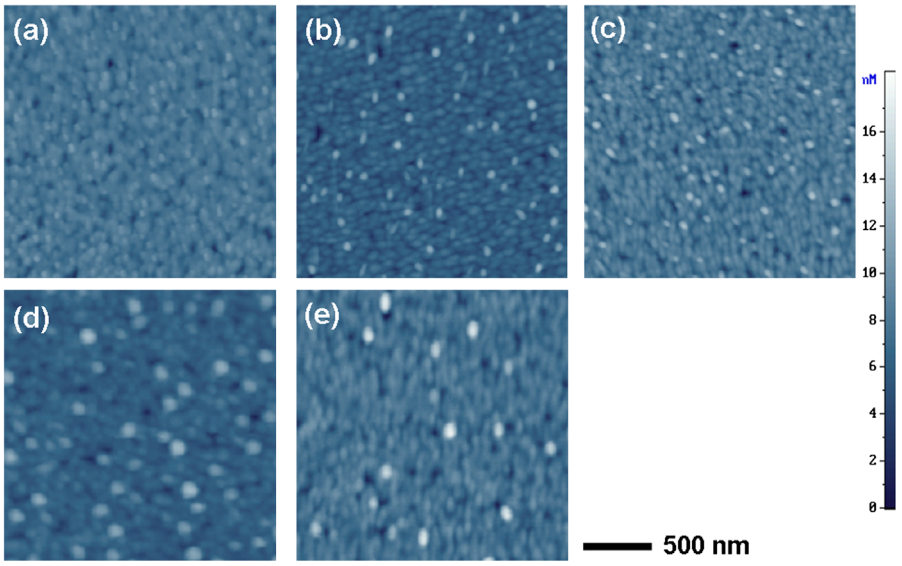


**Fig. 1.** Plan-view atomic force microscopy images with ZnTe coverage of (a) 2.0, (b) 2.2, (c) 2.4, (d) 2.7, and (e) 3.0 ML.

of the scale bar the brightest and darkest indicate the relative height of 18 and 0 nm, respectively. The corresponding dot density as a function of coverage is plotted in Fig. 2. Fig. 1(a) reveals two-dimensional-like (2D-like) plateaus on the 2.0-ML-thick specimen and almost no dots appear. When the coverage increases, three-dimensional (3D) dots appear on 2D-like plateaus with a sharp increase of density as shown in Fig. 1(b) and (c). The rearrangement of ZnTe from 2D-like plateaus to 3D dots was attributed to the Stranski–Krastanov (S–K) process. According to the theoretical simulation [10], the morphology changes because of the minimization of total energy during the heterostructural growth under equilibrium. The total energy includes the surface energy of the deposited material and the strain energy arises from the lattice mismatch. When the lattice mismatch ranges from 6.7% to 7.9% the growth starts in 2D and changes to form 3D dots once the coverage exceeds a transition thickness in the range of 1.5–2.0 ML. In this study a lattice mismatch of 7.4% between ZnTe (lattice constant of 6.102 Å) and $Zn_{0.95}Mn_{0.05}Se$ (lattice constant of 5.679 Å [11]) lies in this predicted regime; hence the S–K process is allowed. The solid line in Fig. 2 represents an experimental description of the coverage $\theta$ dependent dot density $\rho$ following the S–K process [12] as

$$\rho = \rho_S(\theta-\theta_C)^{\alpha}, \quad (1)$$

in which $\rho_S$ is the saturated density, $\alpha$ is the exponent, and $\theta_C$ is the critical coverage of the transition. The best fitted values in our results of $\rho_S$ and $\alpha$ are $7.5\times10^9$ cm$^{-2}$ and 1.4, respectively. The transition coverage is 2.0 ML, which satisfies the theoretical prediction and the AFM image. Additionally, with further increase of coverage the AFM images exhibit a coexistence of large and small dots as shown in Fig. 1(d) and (e), respectively, for the 2.7-ML- and 3.0-ML-thick specimen. The corresponding dot densities are also lower than the predicted values. These phenomena imply the ripened process [10,13], which starts when the coverage exceeds 2.7 ML. Portions of the 3D dots enlarge at the expense of others and result in a coexistence of large and small dots as well as a reduced overall dot density.

In addition to the growth evolution, the optical properties of the capped specimens were also investigated for the basic studies on magneto-optical researches. Fig. 3 shows the PL spectra at 10 K in which two emission bands were observed. The higher-energy band (marked by a dash line and labeled 'H-band') shows no clear

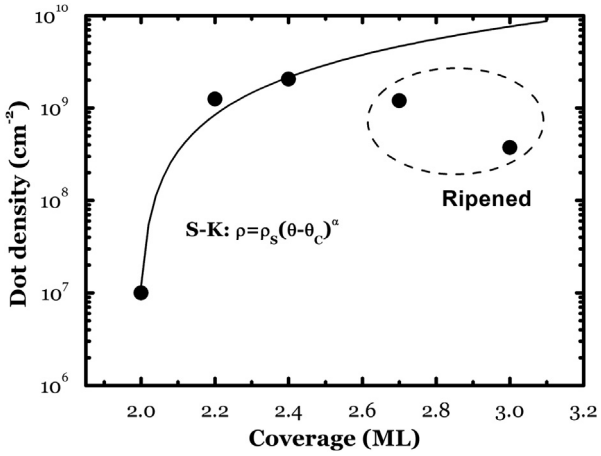


**Fig. 2.** Dot density of ZnTe grown on ZnMnSe as a function of coverage. The solid curve represents the predicted densities by Eq. (1).

energy shift with increasing coverage. The emission could be explained by either the deep-level transition from the buffer layer [14] or the transition from the plateau [15]. On the contrary, the peak positions of the lower-energy band (marked by dash-dot lines) are sensitive to the coverage. The decreasing emission energies together with the increasing coverage, as shown in the inset, were attributed to the reduced quantum confinement of carriers in the ZnTe quantum dots. Therefore the lower-energy emissions were labeled 'QD-band'. Moreover, all of the transition energies of the QD-band are lower than that of the ZnTe epilayer (2.37 eV at 10 K). A type-II band alignment was thus realized in which holes are confined in ZnTe QD while electrons are distributed in the ZnMnSe matrix in the vicinity of the QD and bound to holes via the Coulomb interaction.

In order to demonstrate the magneto-optical characteristics of ZnTe/ZnMnSe QD, the 2.7-ML-thick specimen was chosen because of its strongest emission intensity. The up-polarized (black solid line) and the down-polarized (gray dot line) components of PL spectra at 0 and 4 T are plotted in Fig. 4(a). In the absence of the magnetic field, the intensity of the up-polarized component $I^+$ and the down-polarized one $I^-$ are identical. Hence the degree of circular polarization $P$, which is expressed by $P=(I^+ - I^-)/(I^+ + I^-)$, is zero. On the contrary, a strong circular polarization

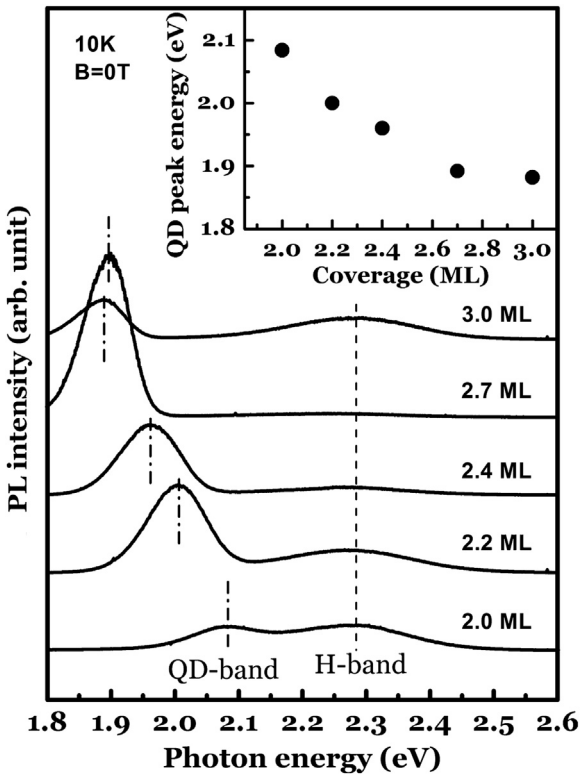


**Fig. 3.** PL spectra at 10 K of ZnTe with different coverage. The inset shows the dependence of corresponding peak position on ZnTe coverage.

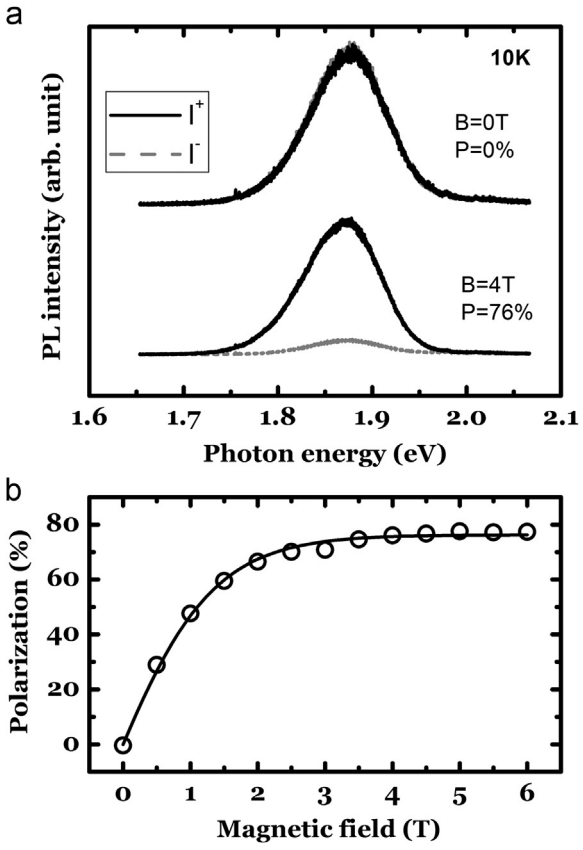


**Fig. 4.** (a) 10 K up-polarized ($I^+$) and down-polarized ($I^-$) PL spectra of QD at $B=0$ and 4 T. (b) The degree of circular polarization as a function of the applied magnetic field.

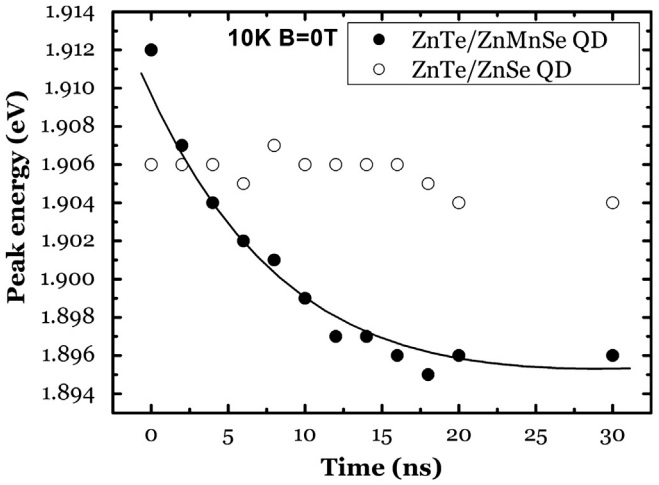


**Fig. 5.** Dependence of PL peak energies at 10 K of ZnTe QD embedded in a ZnMnSe (full circle) and a ZnSe (open circle) matrix.

of 76% at 4 T is observed. In the type-II band structure, the non-zero polarization is owing to the energy splitting of the conduction band in ZnMnSe barrier layer. Transitions between confined holes and electrons which occupy the lower-energy ($m_S=-1/2$) and the higher-energy ($m_S=1/2$) level allows the up-polarized and down-polarized components, respectively. At the low temperature of 10 K, the energy separation of about 5 meV between $I^+$ and $I^-$ promotes electrons to relax to the spin-up level and inhibits the reverse process. Therefore the up-polarized transition dominates. Fig. 4(b) reveals that when the magnetic field increases the degree of circular polarization increases and saturates as the field strength exceeds 4 T. This dependence of the polarization on magnetic field strength is a typical characteristic of diluted magnetic semiconductors.

Furthermore, Fig. 4(a) shows that the splitting is significantly smaller than that observed in the ZnMnSe epilayer with a value of ~80 meV at 4 T [16] while the degree of circular polarization is comparable. Recently, such a paradox has been investigated for the ZnMnTe/ZnSe QD system [17] and been interpreted by the formation of magnetic polarons. During the formation process, the exchange interaction between the localized electrons in the vicinity of QD and Mn ions aligns the randomly oriented spin of Mn ions and reduces the QD-band transition energy. In order to realize the formation of the MP, the time evolution of PL peak position at $B=0$ T was investigated as shown in Fig. 5. The solid circles represent the evolution of the transition energy of QD-band for the 2.7-ML-thick specimen with a red-shift from 1.912 to 1.896 eV within 20 ns. In comparison, ZnTe QD embedded in the non-magnetic ZnSe matrix show no red-shift. Therefore other candidates such as carrier localization and band bending for the temporal evolution of the peak position were excluded. According to previous literatures [18], the formation dynamics could be described by a single exponential law as

$$E(t)=E(t=0)-E_{MP}[1-\exp(-t/\tau_{MP})], \quad (2)$$

in which $E_{MP}$ of 16 meV is the MP binding energy and $\tau_{MP}$ of 7.4 ns is the formation time.

## 4. Conclusion

In this article, the type-II ZnTe/$Zn_{0.95}Mn_{0.05}Se$ single-layer quantum dots were achieved by molecular beam epitaxy. The growth follows the Stranski–Krastanov process with transition coverage of 2.0 ML, whereas the ripened process dominates as

coverage exceeds 2.7 ML. The magneto-optical measurements revealed a saturated degree of circular polarization of quantum dots of 76% at 4 T and the formation of magnetic polarons with binding energy of 16 meV and formation time of 7.4 ns. These approaches provide the evidence of the exchange interaction and the alignment of the randomly oriented Mn spins nearby the QD.

## Acknowledgment

This work was supported by the National Science Council under Grant no. NSC 100-2119-M-009-003.

## References

[1] J.K. Furdyna, Diluted magnetic semiconductors, Journal of Applied Physics 64 (1988) R29–R64.
[2] R. Fiederling, M. Keim, G. Reuscher, W. Ossau, G. Schmidt, A. Waag, L.W. Molenkamp, Injection and detection of a spin-polarized current in a light-emitting diode, Nature 402 (1999) 787–790.
[3] F. Xiu, Y. Wang, J. Kim, P. Upadhyaya, Y. Zhou, X. Kou, W. Han, R.K. Kawakami, J. Zou, K.L. Wang, Room-temperature electric-field controlled ferromagnetism in $Mn_{0.05}Ge_{0.95}$ quantum dots, ACS Nano 4 (2010) 4948–4954.
[4] R. Viswanatha, J.M. Pietryga, V.I. Klimov, S.A. Crooker, Spin-polarized $Mn^{2+}$ emission from Mn-doped colloidal nanocrystals, Physical Review Letters 107 (2011) 067402.
[5] M.C. Kuo, J.S. Hsu, J.L. Shen, K.C. Chiu, W.C. Fan, Y.C. Lin, C.H. Chia, W.C. Chou, M. Yasar, R. Mallory, A. Petrou, H. Luo, Photoluminescence studies of type-II diluted magnetic semiconductor ZnMnTe/ZnSe quantum dots, Applied Physics Letters 89 (2006) 263111.
[6] W.C. Fan, J.T. Ku, W.C. Chou, W.K. Chen, W.H. Chang, C.S. Yang, C.H. Chia, Magneto-optical properties of ZnMnTe/ZnSe quantum dots, Journal of Crystal Growth 323 (2011) 380–382.
[7] H. Mino, Y. Kouno, K. Oto, K. Muro, R. Akimoto, S. Takeyama, Optically induced long-lived electron spin coherence in ZnSe/BeTe type-II quantum wells, Applied Physics Letters 92 (2008) 153101.
[8] E. Oh, K.J. Yee, S.M. Soh, J.U. Lee, J.C. Woo, H.S. Jeon, D.S. Kim, S. Lee, J.K. Furdyna, H.C. Ri, H.S. Chany, S.H. Park, Spin polarization of self-assembled CdSe quantum dots in ZnMnSe, Applied Physics Letters 83 (2003) 4604–4606.
[9] W.K. Hung, M.Y. Chern, Y.F. Chen, W.C. Chou, C.S. Yang, C.C. Cheng, J.L. Shen, Optical properties of $Zn_{1-x}Mn_xSe$ ($x \leqq 0.78$) epilayers, Solid State Communications 120 (2001) 311–315.
[10] I. Daruka, A. Barabási, Dislocation-free island formation in heteroepitaxial growth: a study at equilibrium, Physical Review Letters 79 (1997) 3708–3711.
[11] Y.M. Yu, D.J. Kim, K.J. Lee, Y.D. Choi, O. Byungsung, K.S. Lee, I.H. Choi, M.Y. Yoon, Effect of Mn composition on characterization of $Zn_{1-x}Mn_xSe$ epilayers, Journal of Vacuum Science & Technology A 22 (2004) 1098–1911.
[12] D. Leonard, K. Pond, P.M. Petroff, Critical layer thickness of self-assembled InAs islands on GaAs, Physical Review B 50 (1994) 11687–11692.
[13] S. Lee, I. Daruka, C.S. Kim, A.-L. Barabási, J.L. Merz, J.K. Furdyna, Dynamics of ripening of self-assembled II–VI semiconductor quantum dots, Physical Review Letters 81 (1998) 3479–3482.
[14] T. Yokogawa, M. Ogura, T. Kajiwara, High quality ZnSe films grown by low pressure metalorganic vapor phase epitaxy using methylalkyls, Applied Physics Letters 50 (1987) 1065–1067.
[15] R. Najjar, R. André, L. Besombes, C. Bougerol, S. Tatarenko, H. Mariette, Elaboration and optical properties of type-II ZnTe on ZnSe heterostructures, Materials Science and Engineering B 165 (2009) 85–87.
[16] T. Slobodskyy, C. Rüster, R. Fiederling, D. Keller, C. Gould, W. Ossau, G. Schmidt, L.W. Molenkamp, Molecular-beam epitaxy of (Zn,Mn)Se on Si(100), Applied Physics Letters 85 (2004) 6215–6217.
[17] I.R. Sellers, R. Oszwaldowski, V.R. Whiteside, M. Eginligil, A. Petrou, I. Zutic, W.C. Chou, W.C. Fan, A.G. Petukhov, S.J. Kim, A.N. Cartwright, B.D. McCombe, Robust magnetic polarons in type-II (Zn, Mn)Te/ZnSe magnetic quantum dots, Physical Review B 82 (2010) 195320.
[18] J.H. Harris, A.V. Nurmikko, Formation of the bound magnetic polaron in (Cd, Mn)Se, Physical Review Letters 51 (1983) 1472–1475.